PHYSICAL REVIEW B VOLUME 57, NUMBER 19 15 MAY 1998-I

Potential role of silanones in the photoluminescence-excitation, visible-photoluminescence-emission, and infrared spectra of porous silicon

James L. Gole
School of Physics, Georgia Institute of Technology, Atlanta, Georgia 30332

David A. Dixon
Environmental Molecular Sciences Laboratory, Pacific Northwest National Laboratory, P.O. Box 999, K1-83, Richland, Washington 99352

(Received 28 April 1997; revised manuscript received 5 January 1998)

Ab initio molecular electronic structure calculations on select silanones, silylenes, and tricoordinated silicon compounds SiXYZ with a dangling electron are presented. The calculations are used to evaluate the nature of the electronic spectra, which are to be associated with surface-bound Si/O/H compounds. In concert, they are used to suggest an explanation for the nature of the photoluminescence-excitation spectrum (PLE) and the subsequent visible luminescence (PL) from porous silicon (PS) based on the optical properties of the silanone-based oxyhydrides. In order to make this selection, we treat a set of compounds that includes the silanones $Si(O)H_2$, $Si(O)H(OH)$, $Si(O)(OH)_2$, $Si(O)H(OSiH_3)$, $Si(O)H(SiH_3)$, $Si(O)(OH)(SiH_3)$, $Si(O)(SiH_3)_2$, and $Si(O)(SiH_3)(OSiH_3)$, the silylenes HSiOH, HOSiOH, and $HOSiOSiH_3$, and the tricoordinated silicon compounds SiH_3, $Si(OH)H_2$, $Si(OH)_2H$, and $Si(OH)_3$. The silanone-based oxyhydride structures containing either an OH or $OSiH_3$ group all display adiabatic ground-state singlet-excited-state triplet exciton separations in the range close to 400 nm. This adiabatic energy is consistent with the vertical transition energies associated with the PS excitation spectrum (PLE) as a large change in the Si═O bond distance (~ 0.17 Å) accompanies the transition from the silanone ground electronic singlet state to the low-lying triplet exciton (or its closely lying singlet coupled configuration). The maximum in the PLE spectrum, obtained through optical pumping from the lowest vibrational levels of the ground electronic state to considerably higher levels of the triplet exciton electronic state, should therefore be shifted to considerably shorter wavelength consistent with an absorption spectrum peaking at 350 nm as observed by several researchers. A shift to larger internuclear distance in the excited-state triplet exciton will also produce a considerable redshift in the PL emission spectrum relative to the absorption-excitation wavelengths, again consistent with experimental observation. The calculated IR spectra for the *silanone-based* oxyhydrides are also consistent with the observed Fourier transform IR spectra of porous silicon. In clear contrast, neither the silylenes nor the tricoordinated silicon compounds with dangling electrons can account for the excitation or emission features that are associated with PS as their lowest-lying transitions result in minimal changes in bonding and/or occur at much higher energy (shorter wavelength). The results obtained in this study also suggest that surface passivation or the saturation of valency is incommensurate with the formation of the fluorophors that will produce the emission from PS. [S0163-1829(98)08619-6]

I. INTRODUCTION

Electrochemically etched highly porous silicon (PS) wafers have been the subject of great interest due to their room-temperature visible-light emission observed as photoluminescence (PL) upon excitation (PLE) with an appropriate light source.[1–3] While the PLE (absorption) spectrum of a prepared PS sample in air peaks at $\sim$350 nm, the resulting visible PL spectrum occurs at considerably longer wavelength. Under the appropriate conditions, PS first displays an *in situ* ‘‘green’’ luminescence[4,5] ($\sim$500–600 nm) during the early and intermediate stages of the etching process. The green luminescence then transforms to a final ‘‘orange-red’’ luminescence (600–800 nm) although it can be stabilized for extended periods with appropriate solvation.[4,5] An intense research effort over the past five years has focused on establishing the origin of this luminescence associated with a PS emitter. Here, we examine the potential role of select surface-bound silicon oxyhydrides as a source of the PL emission from porous silicon.

It is believed that the luminescence from PS occurs at or near the silicon surface. The efficiency and wavelength range of the emitted light is strongly affected by the physical and electronic structure of the surface and, for *in situ* observations, by the nature of the etching process.[3,5] However, the source of the PS luminescence is controversial. One popular hypothesis asserts that the luminescence results from the radiative recombination of quantum-confined electrons and holes in columnar structures or undulating wires.[6–9] Supporting *prima facie* evidence for this model comes from Calcott *et al.*,[6] who have reported phonon-assisted radiative processes involving those phonons that are necessary to couple the electron valley states in crystalline silicon near the X point, to Γ point hole states. Shuppler and co-workers,[10,11] while questioning the existence of columnar structures or undulating wires, have reported on the size, shape, and composition of luminescent species in oxidized silicon nanocrystals, correlating their results with data on hydrogen-passivated PS and also suggesting a quantum confinement model. A second explanation has focussed on the importance of surface localized states, involving irregularly shaped small crystallites that are not perfectly passivated, wherein elementary excitations are first trapped prior to recombination.[12,13] In analogy with the well-studied luminescence from amorphous silicon (a-Si-H),[14] the carriers, in the bound states associated with reconstructed and disordered silicon in the boundary layer, are thought to recombine radiatively.

Yet a third explanation for the visible emission from porous silicon contends that the luminescence results from the presence of surface-confined molecular emitters. These include polysilane[15] formed in the internal surface of the pores or a molecular complex of silicon, oxygen, and hydrogen known as siloxane ($Si_6O_3H_6$) and its derivatives.[16–18] By using the optical detection of magnetic resonance (ODMR), Stutzmann and co-workers[16–18] have clearly established that the PS ''red'' emission results from a triplet state (triple exciton) that is thought to phosphoresce. It is the close analogy of both the ODMR and optical excitation (PLE) and photoluminescence spectra of PS and ''annealed'' siloxane that led Stutzmann and co-workers[16–18] to suggest this molecule as the origin of the PS photoluminescence. While this *prima facie* evidence is enticing, it may suggest a more general origin for the observed features in the form of the fluorophors correlated with the formation of an $Si{=}O$ bond[19] and associated with the silicon oxyhydrides formed and bound to the PS surface. These bound oxyhydride fluorophors are to be distinguished from surface adsorbates.[20] In fact, Steckl *et al.*[21] have obtained evidence for the presence of the silicon oxyhydrides in stain etched porous silicon thin films, correlating their observations with crystallinity and photoluminescence. Further, in a study of the thermal oxidation and nitrogen annealing of luminescent PS, Yan *et al.*[22] have obtained evidence that residual hydrogen exists in a 1000 °C/10 min thermally oxidized PS film at least in the form of SiOH.

We have carried out an extensive series of experiments[5,19,23–25] evaluating the *in situ* PL in both aqueous and nonaqueous media and establishing conditions under which the porous silicon PL is stabilized,[5,26] enhanced,[5] or quenched.[5] These studies, coupled with the range of quantum chemical calculations that we discuss below, suggest[24] that the source of the PS photoluminescence might well correspond to a silanone-based silicon oxyhydride strongly bound to the PS surface. The detailed quantum chemical modeling that we report encompasses a sufficient set of compounds so as to suggest a plausible and close correlation between the manifold of silicon oxyhydride triplet (and singlet) excited states and the observed *in situ* green and final orange-red PL spectra characteristic of PS. The demonstrated changes in bonding associated with electronic transitions involving these silanone-based oxyhydrides, especially the changes in the SiO-related bonds in transition, can readily explain the observed character of the PL spectra.

We find that the major changes associated with the lowest-energy transitions of these silicon oxyhydrides, especially those from the ground-state singlet to the lowest-lying excited triplet state, involve a significant lengthening of the Si-O bond. We demonstrate that the more commonly observed orange-red PL spectrum can result from silanone-based oxyhydride structures containing either an -OH or $OSiH_3$ functional group. These silanones, in particular, are found to display an adiabatic ground-state singlet excited-state triplet exciton separation corresponding to $\lambda_{\text{adiabatic}}$ $\sim$400 nm. Because of the substantial change in the $Si{=}O$ bond distance, the peak in the PLE excitation spectrum, involving significantly higher excited-state vibrational levels, should be shifted to considerably shorter wavelength, consistent with the $\sim$350-nm peak in the experimentally observed[27] spectrum for PS. In fact, the large shift in the excited-state potentials relative to the ground state is also consistent with a significant difference in the peak of the PLE excitation spectrum ($\sim$350 nm) and the observed PL emission range (600–800 nm). It is considered significant that the locations of the unsaturated silanone-based oxyhydride triplet states and the known peak wavelength of the porous silicon (PLE) excitation spectrum ($\sim$350 nm) (Ref. 27) bear a clear resemblance to the known singlet-triplet splittings of the low-lying silicon monoxide intercombination band systems.[28]

In order to better understand the electronic spectra of the silicon oxyhydrides and to obtain a sufficient data set that can be used to examine their close correlation with the visible luminescence from porous silicon, we have extended three previous studies[29–31] of the molecular electronic structure of silanone [$Si(O)H_2$] and the OH (for H) substituted silanoic [$Si(O)H(OH)$] and silycic [$Si(O)(OH)_2$] acids. Here, in order to obtain a more complete model, we include in our study the silanone-based $Si(O)H(OSiH_3)$, $Si(O)H(SiH_3)$, $Si(O)(OH)(SiH_3)$, $Si(O)(SiH_3)(OSiH_3)$, and $Si(O)(SiH_3)_2$ constituencies as models for sites present on the surface of an etched silicon wafer, comparing the distinct behavior of these compounds to the appropriate silylene isomers. In the course of this study, we have also examined structures involving a tricoordinated silicon with a dangling electron (singly occupied orbital), including SiH_3, $Si(OH)H_2$, $Si(OH)_2H$, and $Si(OH)_3$. We will establish that the analogs of these latter compounds and the silylenes as surface bound fluorophors cannot contribute to the observed PS photoluminescence.

II. DETAILS OF THE CALCULATIONS

We have considerably expanded our previous calculations,[29,30] which were limited by available computational resources to moderate-size basis sets. In the present study, we employ both *ab initio* molecular-orbital theory and density-functional theory (DFT). The calculations have been done with the program systems DGauss[32] (DFT calculations) and Gaussian 94 (Ref. 33) (*ab initio* MO calculations). The molecules $Si(O)H_2$, $Si(O)H(OH)$, $Si(O)(OH)_2$, $Si(O)H(OSiH_3)$, $Si(O)H(SiH_3)$, $Si(O)(OH)(SiH_3)$, $Si(O)(SiH_3)(OSiH_3)$, and $Si(O)(SiH_3)_2$ were used as models for the types of sites that would be expected to be present on a hydrogen-passivated silicon surface[34] undergoing oxidation. Although cluster models such as these do not include the long-range Coulomb effects present in the bulk, they do provide useful insights into the effect of changing the functional groups that are attached to the silicon.

Geometries for the ground-state singlet structures were initially optimized by using polarized triple ζ valence basis sets[35] at the local DFT level. Second derivative calculations[36] on the optimized structures showed them to be minima. Geometries for the first excited triplet state of a selection of the

TABLE I. $Si(O)H_2$ optimized geometry parameters. Bond distances in Å and bond angles in degrees.

Molecule	Method	r(Si═O)	r(Si-H)	<(H-Si-H)	<(H-Si-O)
Ground state	MP2/DZP	1.545	1.470	111.2	124.4
Ground state	LDFT/TZVP	1.534	1.505	112.3	123.9
Excited triplet	MP2/DZP	1.700	1.478	111.8	105.6
Excited singlet	MP2/DZP	1.705	1.476	112.2	106.0
Excited triplet	LDFT/TZVP	1.626	1.546	102.9	102.0

molecules considered were also optimized at this level. The optimum DFT geometries were then used in molecular-orbital calculations at the MP2 level[37] with a polarized double ζ basis set.[38] The geometries were again optimized at the MP2/DZP level and frequency calculations were done for these optimized geometries. The open shell *ab initio* MO calculations were carried out using the UHF formalism.

Higher-order correlation calculations were done on $Si(O)H_2$ at the optimized geometries. These calculations were done at the CCSD(T) level[39] with a triple ζ basis set[40] augmented by two sets of polarization functions on all atoms and by f functions on the heavy atoms.

III. RESULTS

A. Evaluation of calculated structures

Geometries of ground-state structures. The important geometric parameters for the ground electronic state and low-lying electronic states of silanone are summarized in Table I. The Si═O bond lengths of the ground and excited triplet states of the various silanones are given in Table II. Details of the geometries of the remaining species are given as supplementary material (see Ref. 71). The optimized structures are depicted in Fig. 1.

Effect of change in substituent bound to silicon on the ground-state Si═O bond. We first consider (Table II) the effect which the changing of a substituent on the silicon has on the Si═O bond length. The substitution of an OH or $OSiH_3$ for hydrogen (H) produces an ~0.008 Å decrease in the Si═O bond length while substitution of a second OH or $OSiH_3$ produces no significant change. The replacement of hydrogen with SiH_3 produces a lengthening of the Si═O bond and the combined effect of replacing one H by OH and the other by SiH_3 leads to a near cancellation of the effects due to the substituent. There is essentially no effect on the Si═O bond length if the H in an OH group is substituted by an SiH_3 group. The results obtained by using a local-density-functional treatment (LDFT) are similar to those obtained at the MP2 level with the Si═O bond found to be ~0.01 Å shorter at the LDFT/TZVP level. The Si═O bond lengths determined at the MP2 level are shorter than Si-O single bonds to sp^2 or sp^3 Si by ~0.1 and 0.15 Å, respectively. The LDFT calculations indicate similar trends.

Formation of excited triplet state—validity of the LDFT method. In order to examine the nature of the geometry changes that occur on formation of the excited triplet state, we focus on the model compound $Si(O)H_2$. We find that the formation of the first excited triplet ($^3A''$) state of this molecule leads to a significant increase in the Si═O bond length to 1.700 Å (Table I—MP2/DZP). The silanone molecule is no longer planar with C_{2v} symmetry but now has a pyramidal structure with only C_s symmetry (Fig. 1). The O-Si-H bond angle closes down by almost 20° from 124.4° to 105.6° in the triplet. In contrast, the H-Si-H bond angle shows essentially no change in the transition from the singlet to the triplet. The change in Si-O bond length, which is a significant 0.15 Å, is consistent with the formation of a Si atom with sp^3-type bonding and compares with predictions for a single Si-O bond in compounds with an SiH_3O group (see supplementary material[71]). Only a slight increase in the Si-H bond length is predicted as the triplet is formed.

The results obtained for the low-lying $^3A''$ state of silanone at the LDFT level (Table I-LDFT/TZVP) predict a considerably different structure. The Si═O bond is found to lengthen by only 0.09 Å and appears to be more like an Si-O single bond to an sp^2 Si. The Si—H bonds show a significant 0.04 Å increase. The calculated bond angles at the two levels of calculation also show significant differences. The H-Si-O bond angles at the LDFT level are smaller than those predicted by the *ab initio* MO results by 3.7° and the calculated H-Si-H angle is 10° smaller at the LDFT level. *This suggests that the LDFT method is not predicting a reliable structure for the geometries of the triplet states of these species.*

Low-lying excited singlet state of silanone. As we have discussed previously,[29] there is a $^1A''$ excited state that lies a few kcal/mol above the $^3A''$ state with the same basic electronic configuration. Geometry optimization of the $^1A''$ excited state at the MP2/DZP level (Table I) yields a structure that is essentially the same as the triplet structure. The largest geometry change corresponds to the Si-O bond, which increases by 0.005 Å as compared to the triplet.

Transformation to silylene isomers. Previously,[29] we indicated concern with the nature of the silylene isomer, HSiOH, and where it lies energetically with respect to various states in the $Si(O)H_2$ manifold. However, we were not able to obtain a reliable energy difference between the two isomers nor were we able to calculate the vibrational frequencies to establish the geometry of the silylene. We have now optimized the geometries of the silylenes obtained from several silanones by a rearrangement that leads to the insertion of oxygen (O) into either an Si-H or Si-Si bond, forming the Si-OH or Si-OSi bonds. The insertion into an Si-O to form an O-O bond was not studied as this leads to the formation of a higher-energy peroxide. The lowest-energy configuration of the silylenes is a singlet and we have optimized both this ground-state singlet and the first excited state triplet at the MP2/DZP levels. The geometry of the singlet ground-state

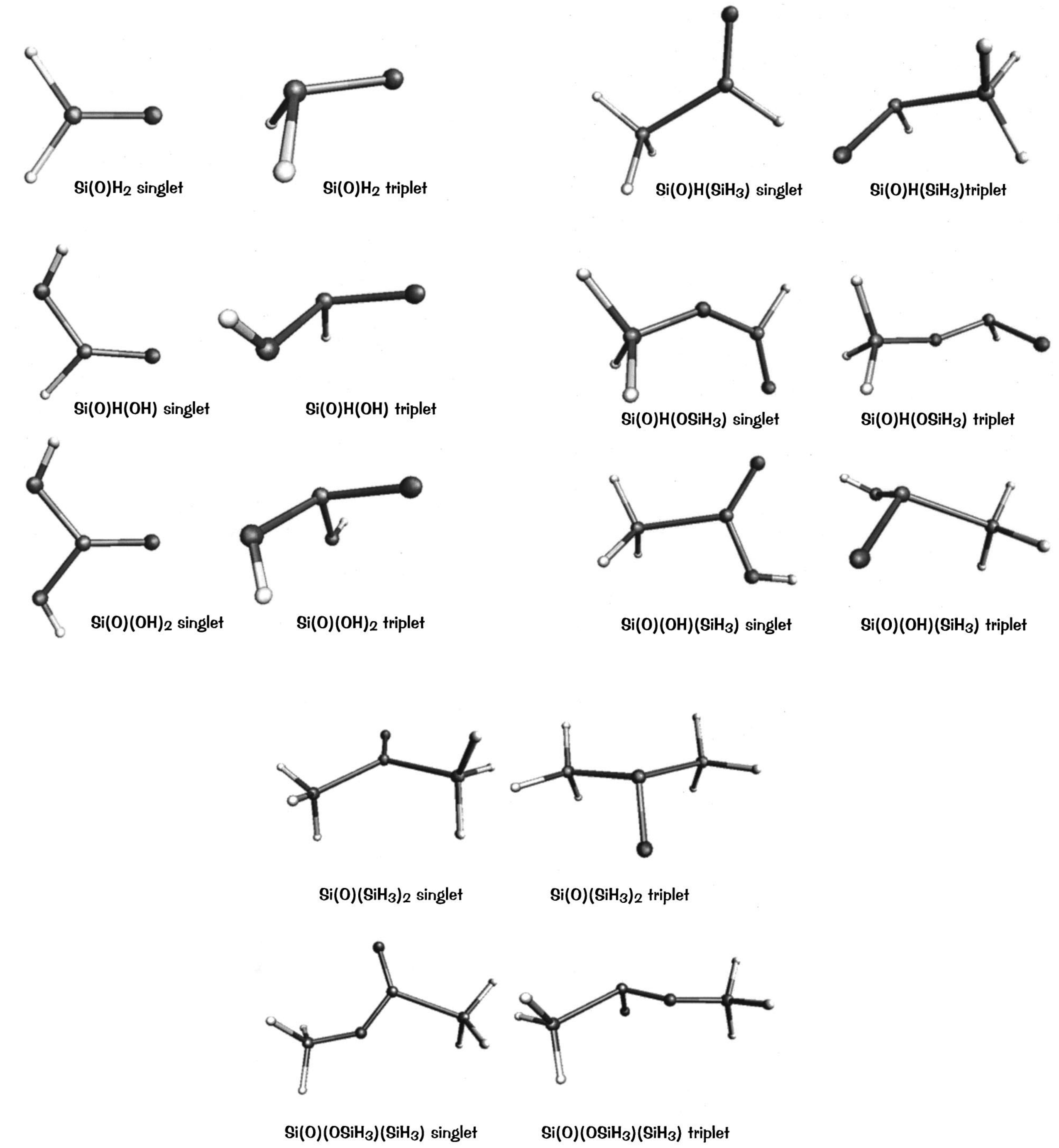

Si(O)H_2 singlet

Si(O)H_2 triplet

Si(O)H(SiH_3) singlet

Si(O)H(SiH_3)triplet

Si(O)H(OH) singlet

Si(O)H(OH) triplet

Si(O)H($OSiH_3$) singlet

Si(O)H($OSiH_3$) triplet

Si(O)$(OH)_2$ singlet

Si(O)$(OH)_2$ triplet

Si(O)(OH)(SiH_3) singlet

Si(O)(OH)(SiH_3) triplet

Si(O)$(SiH_3)_2$ singlet

Si(O)$(SiH_3)_2$ triplet

Si(O)($OSiH_3$)(SiH_3) singlet

Si(O)($OSiH_3$)(SiH_3) triplet

FIG. 1. DZP/MP2 optimized geometries for ground-state and first excited triplet state silanones.

HSiOH is planar with C_s symmetry. The Si-O bond length is 1.680 Å and is much like an Si-O single bond to an sp^3 Si. The H-Si-O bond angle is 94.4°, consistent with that expected for a singlet silylene (90°).[41] The Si-H bond length is 1.509 Å, almost 0.04 Å longer than the bond length in Si(O)H_2. The geometry of the triplet is not planar but has an H-Si-O-H dihedral angle of 94.2°. The H-Si-O angle increases to 117.3°, as expected in the formation of triplet silylene. The Si-O bond length remains essentially the same as that in the singlet while the H-Si bond length is only 0.008 Å longer than that in Si(O)H_2. The rotated triplet is 2.4 kcal/mol more stable than the planar triplet at the UMP2/DZP level.

Two other silylenes were studied. They are HOSiOH and $HOSiOSiH_3$, which can be formed from either Si(O)H($OSiH_3$) or from Si(O)(OH)(SiH_3). Both these silylenes in the triplet state have dihedral angles about the Si-O bonds close to 90°.

Si═O bond lengths in the excited state of silanone. We have evaluated the Si═O bond lengths for the silanones and their substantial increase in the transition from the ground-state singlet to the lowest-lying triplet state. These results are summarized in Table II. By far the largest change in bond length during transition occurs for the Si═O bond. By contrast, Table III demonstrates much smaller changes for the Si-Si bond lengths of the appropriate compounds.

TABLE II. Si═O bond lengths (Å) for silanones at the MP2/DZP level.

Molecule	r(Si—O) singlet	r(Si—O) triplet	Δr(Si—O)
$Si(O)H_2$	1.545	1.700[a]	0.155
Si(O)H(OH)	1.537	1.709	0.172
$Si(O)(OH)_2$	1.536	1.709	0.173
$Si(O)H(OSiH_3)$	1.537	1.708	0.171
$Si(O)H(SiH_3)$	1.553	1.695	0.142
$Si(O)(OH)(SiH_3)$	1.543	1.712	0.169
$Si(O)(SiH_3)_2$	1.560	1.681	0.121
$Si(O)(OSiH_3)(SiH_3)$	1.543	1.712	0.169

[a] Bond length for the excited singlet is 1.705 Å. See text for discussion.

Because of the problems inherent in the LDFT description of the $Si(O)H_2$ triplet state, we discuss only the results of geometry optimizations for the remaining triplets at the MP2 level. The optimized geometries all demonstrate that the original Si═O bond is significantly lengthened in the triplet. Rather than the shortening of the Si═O bond predicted for the ground state, the substitution of H by OH or $OSiH_3$ leads to an increase in this bond close to 0.01 Å over that in the triplet of $Si(O)H_2$. The substitution of SiH_3 for H does lead to a slightly shorter Si-O bond by about 0.005 Å, in $Si(O)HSiH_3$ and by 0.02 Å in $Si(O)(SiH_3)_2$. Thus, if the silicon is bonded to an oxygen, the change in the Si═O bond length on excitation is larger than if the silicon is bonded to hydrogen or silicon.

B. Energetics

Evaluation of ground-state–excited triplet separations for $Si(O)H_2$. In order to evaluate the predicted singlet-triplet transition energy for the variety of species considered in this study and to establish the validity of the energies calculated for the singlet and triplet states, we improved the level of correlation treatment (n-particle space) for $Si(O)H_2$ to CCSD(T) and the basis set (one-particle space) to triple ζ with two additional polarization functions (TZ2PF). The total energies are given in Table IV whereas scaled energy differences, as discussed below, are given in Table V.

TABLE III. Si-Si bond lengths (Å) for silanones at the MP2/DZP level.

Molecule	r(Si-Si) singlet	r(Si-Si) triplet	Δr(Si-Si)
$Si(O)H(SiH_3)$	2.354	2.361	0.007
$Si(O)(OH)(SiH_3)$	2.342	2.365	0.023
$Si(O)(SiH_3)_2$	2.366	2.363	−0.003
$Si(O)(OSiH_3)(SiH_3)$	2.341	2.373	0.032

We predict that the $H_2Si(O)$ triplet lies 61.1 kcal/mol (2.65 eV) above the ground-state singlet with calculations done at the CCSD(T)/TZ2PF level. This should be compared to 66.1 kcal/mol (2.87 eV) and 67.1 kcal/mol calculated at the MP2/DZP level with and without spin projection.[42] Thus the lower-level calculations provide a reasonable estimate of the singlet-triplet excitation energy and can be used to suggest regions where the singlet-triplet absorption (PLE) and emission (PL) spectra should be observed.

Some insight into the effective cancellation of errors for the singlet-triplet separation at the MP2/DZP level of description can be obtained by comparing the various splittings at different correlation levels for larger basis sets. The MP2/TZ2PF [$\Delta E(S\text{-}T) = 71.6$ kcal/mol) and PMP2/TZ2PF [$\Delta E(S\text{-}T) = 70.2$ kcal/mol) energy differences are actually larger than the MP2/DZP value. The MP4SDQ/TZ2PF value

TABLE IV. Total energies (a.u.) for silanones and silylenes.

	MP2/DZP			
Molecule	E (singlet)	E (triplet) UMP2	E (triplet) PMP2	ΔZPE[a]
$Si(O)H_2$[b]	−365.221408	−365.114467	−365.116249	1.04
Si(O)H(OH)	−440.350361	−440.225566	−440.227363	1.44
$Si(O)(OH)_2$	−515.468765	−515.342779	−515.344503	2.05
$Si(O)H(SiH_3)$	−655.398781	−655.296428	−655.298534	0.73
$Si(O)H(OSiH_3)$	−730.563994	−730.442303	−730.444090	1.26
$Si(O)(OH)(SiH_3)$	−730.530277	−730.404778	−730.406914	1.32
$Si(O)(SiH_3)_2$	−945.578548	−945.481976	−945.484351	0.35
$Si(O)(OSiH_3)(SiH_3)$	−1020.744757	−1020.621996	−1020.624170	1.16
HSiOH	−365.218479	−365.161362	−365.161872	0.61
$Si(OH)_2$	−440.356398	−440.259291	−440.259873	0.25
SiH_3OSiOH	−730.575351	−730.473305	−730.473843	0.31

	CCSD(T)/TZ2PF		
Molecule	E (singlet)	E (triplet)	E (excited singlet)
$Si(O)H_2$	−365.354 035	−365.256 633	−365.252 546
HSiOH	−365.358 493	−365.295 648	

[a] Zero-point energy difference between the singlet and the triplet in kcal/mol.

[b] $Si(O)H_2$ (excited singlet) UMP2 = −365.110 343; PMP2 = −365.117 422; ΔZPE = 0.74 kcal/mol.

TABLE V. Ground-state singlet-excited triplet energy separations $[\Delta E(S\text{-}T)]$ for silanones. See footnote a.

Molecule	$\Delta E(S\text{-}T)$ kcal/mol	$\Delta E(S\text{-}T)$ eV	$\sim\lambda_{\text{Adiabatic}}$ (nm)
$Si(O)H_2$[a]	60.1	2.65	475
$Si(O)H(OH)$[a]	70.9	3.07	403
$Si(O)(OH)_2$[a]	71.0	3.08	402
$Si(O)H(OSiH_3)$[a]	70.3	3.05	406
$Si(O)(OH)(SiH_3)$[a]	71.2	3.09	401
$Si(O)H(SiH_3)$[a]	57.3	2.48	499
$Si(O)(SiH_3)_2$[a]	53.9	2.34	530
$Si(O)(SiH_3)(OSiH_3)$[a]	69.6	3.02	411
HSiOH[b]	38.4	1.66	744
$Si(OH)_2$[b]	64.2	2.78	445
SiH_3OSiOH[b]	67.3	2.92	424

[a] Calculated at the spin projected MP2/DZP level including zero-point energy corrections. A correction factor of −4.9 kcal/mol was applied to the MP2/DZP energy splittings based on the CCSD(T)/TZ2PF calculations of $\Delta E(S\text{-}T)$ for $Si(O)H_2$.

[b] Calculated at the spin projected MP2/DZP level including zero point energy corrections. A correction factor of 3.9 kcal/mol was applied to the MP2/DZP energy splittings based on the CCSD(T)/TZ2PF calculations of $\Delta E(S\text{-}T)$ for HSiOH.

$[\Delta E(S\text{-}T)=61.0$ kcal/mol) is almost the same as the CCSD(T)/TZ2PF value whereas the CCSD/TZ2PF value $[\Delta E(S\text{-}T)=57.7$ kcal/mol) is 3.4 kcal/mol too low. The vibrational correction to the $^3A''-{}^1A''$ energy difference is 1.0 kcal/mol, lowering the splitting, so that the adiabatic energy difference is 60.1 kcal/mol corresponding to a transition wavelength of 475 nm. The singlet-singlet vibrational correction is 0.8 kcal/mol giving an adiabatic energy difference of 62.9 kcal/mol which corresponds to a transition wavelength of 454 nm. In contrast to our previous calculations,[29] where we predicted a $^3A''\text{-}^1A''$ energy difference of 4.6 kcal/mol, the $H_2Si(O)$ excited-state singlet is predicted to be 2.6 kcal/mol (∼0.1 eV) above the triplet at the CCSD(T)/TZ2PF level of description. A similar difference of 2.6 kcal/mol is predicted at the UMP2/DZP level although the use of spin projection[42] at the MP2 level predicts that the singlet lies below the triplet. This indicates that the spin projection approximation should not be used to evaluate the excited singlet-triplet splitting.

Relative energetics of the silanone $[H_2Si(O)]$ and silylene (HSiOH) isomers. Although we were unable previously[29] to establish the energy difference between the silylene and silanone isomers, we can now reliably predict this energy difference. Singlet silylene HOSiH, is predicted to be 2.8 kcal/mol more stable than silanone $Si(O)H_2$ at the CCSD(T)/TZ2PF level. If we include a zero-point correction, we lower this difference to 1.2 kcal/mol or 420 cm^{-1}. The MP2/DZP energies differ by ∼1.8 kcal/mol predicting the silanone to be slightly more stable than the silylene. At the MP2/TZ2PF level, the silanone is again predicted to be 1.8 kcal/mol more stable than the silylene. Calculations at the MP4SDQ/TZ2PF level suggest a 2.6 kcal/mol separation, essentially the same as the CCSD(T) description. The CCSD result, 4.4 kcal/mol, favors the silylene by too great an extent. The stability of the silylene results from the stability of the Si-O and O-H single bonds. These should be compared to the stability of the Si═O π bond and the Si-H bond in silanone. Because the former bonds are significantly stronger than the latter, the formation of silylene is slightly favored.

The silylene triplet is predicted to lie only 39.4 kcal/mol (∼1.7 eV) above ground-state singlet silylene at the CCSD(T)/TZ2PF level. This is consistent with the energy differences observed in other silylenes.[41] The zero-point correction is 1.1 kcal/mol, which lowers the singlet-triplet splitting to 38.4 kcal/mol. This corresponds to a transition wavelength near 744 nm. The silylene triplet is 37.2 kcal/mol above the silanone ground-state singlet, suggesting an adiabatic transition wavelength near 768 nm. The MP2/DZP singlet-triplet energy difference is 35.5 kcal/mol, again in reasonable agreement with the more accurate calculations.

Relative energetics of silanoic acid [Si(O)H(OH)] and HOSiOH. Silanoic acid is obtained by the substitution of OH for H in silanone. The calculated singlet-triplet excitation energies for silanoic acid are 78.3 kcal/mol at the UMP2/DZP level, 77.2 kcal/mol at the PMP2/DZP level, 81.4 kcal/mol at the PMP2/TZ2PF level, and 72.1 kcal/mol at the MP4SDQ/TZ2PF level. We apply a correction factor from the calculations on $Si(O)H_2$ based on the energies calculated at the PMP2/DZP and CCSD(T)/TZ2PF levels of description. This value of 4.9 kcal/mol applied to Si(O)H(OH) suggests a singlet-triplet splitting of 72.3 kcal/mol in good agreement with the calculated MP4SDQ/TZ2PF value. The zero-point correction [Δ(ZPE)] is 1.44 kcal/mol suggesting a final energy difference of 70.9 kcal/mol which corresponds to a transition wavelength of ∼403 nm. We can also estimate that the transition to the excited singlet will be at ∼382 nm [using the excited singlet-triplet splitting of 2.6 kcal/mol from the CCSD(T)/TZ2PF calculation on $Si(O)H_2$].

We find that the silylene, HOSiOH, is more stable than the silanone Si(O)H(OH) by 3.8 kcal/mol at the MP2/DZP level. The Δ(ZPE) correction of 1.2 kcal/mol lowers the energy difference to 2.6 kcal/mol. For HSiOH and $Si(O)H_2$, the difference between the MP2/DZP and CCSD(T)/TZ2PF values is 4.6 kcal/mol. This suggests that the MP2/DZP level of description underestimates the stability of the silylene. Thus, we suggest that the silylene HOSiOH is 7.2 kcal/mol (2520 cm^{-1}) more stable than the silanone Si(O)H(OH). The singlet-triplet splitting in the silylene is 60.9 kcal/mol (2.64 eV) at the UMP2/DZP level and 60.6 kcal/mol at the PMP2/DZP level. The inclusion of zero-point effects will lower this difference by only 0.25 kcal/mol. Again it is important to note that the triplet is not planar. Thus the singlet-triplet energy difference is notably larger than the splitting in HSiOH consistent with the singlet-triplet energy differences predicted[41] for HSiF (37.7 kcal/mol) and SiF_2 (73.5 kcal/mol). By using the MP2-CCSD(T) difference of 3.9 kcal/mol found for HSiOH, we estimate that the singlet-triplet energy difference is 64.2 kcal/mol, corresponding to a transition wavelength of ∼445 nm. With these estimated values, we predict the singlet silanone to triplet silylene transition at ∼501 nm (57 kcal/mol≈2.47 eV) and the singlet silylene to triplet silanone transition at ∼366 nm (78 kcal/mol≈3.38 eV).

Energetics of $Si(O)(OH)_2$. The substitution of a second OH group for H to form $Si(O)(OH)_2$ does not substantially change the singlet-triplet splitting. The triplet is predicted to be 78.0 kcal/mol above the singlet and the Δ(ZPE) correction lowers this energy to 75.9 kcal/mol. Applying a correction factor of 4.9 kcal/mol to the singlet-triplet splitting as described above, we predict a wavelength of ∼402 nm for the singlet-triplet transition. By applying a correction factor of 2.6 kcal/mol, we predict the singlet-singlet transition wavelength at ∼388 nm. The calculated values are similar to those for silanoic acid suggesting that the dominant effect on the transition energy results from the first OH substituent. Because the formation of the silylene results in the creation of a weak peroxide bond, we have not examined this structure.

Energetics of $Si(O)H(OSiH_3)$ *and* $Si(O)(OH)(SiH_3)$ *and conversion to the silylene isomer* (SiH_3OSiOH). In order to better model what might be occurring on a porous silicon we have substituted SiH_3 for H to form $Si(O)H(OSiH_3)$ and $Si(O)(OH)(SiH_3)$. These isomers differ in energy by 21.2 kcal/mol at the MP2/DZP level. The zero-point energy correction increases this to 21.8 kcal/mol with the lower-energy isomer being $Si(O)H(OSiH_3)$, the compound that does not possess a Si-Si bond. For $Si(O)H(OSiH_3)$ the triplet is 75.2 kcal/mol above the singlet at the MP2/DZP level with the zero-point correction lowering this to 74.0 kcal/mol. If we again use a correction factor of 4.9 kcal/mol, the energy of the triplet is predicted to be 70.3 kcal/mol, corresponding to a transition wavelength of ∼406 nm. By using an excited singlet-triplet splitting of 2.6 kcal/mol (from above), we suggest a wavelength of ∼392 nm for the singlet-singlet transition. For $Si(O)(OH)(SIH_3)$, the triplet is 77.4 kcal/mol above the singlet. The zero-point correction lowers this to 76.1 kcal/mol. The 4.9 kcal/mol correction factor leads us to predict that the singlet-triplet transition wavelength is ∼401 nm. The singlet-singlet transition wavelength is estimated at ∼387 nm (using a 2.6 kcal/mol correction).

These two silanone isomers both isomerize to the same silylene, SiH_3OSiOH. The silylene is again predicted to be more stable than either of the silanone isomers. The silylene is more stable than $Si(O)H(OSiH_3)$ by 7.1 kcal/mol at the MP2/DZP level. This reduces to 5.8 kcal/mol if zero-point effects are included. The isomer, $Si(O)(OH)(SiH_3)$, is 28.3 kcal/mol less stable than the silylene. Zero-point effects lower this difference to 27.6 kcal/mol. The silylene triplet lies 63.7 kcal/mol above the ground singlet. This reduces to 63.4 kcal/mol when zero-point effects are included. We apply a correction factor of 3.9 kcal/mol based on the CCSD(T)-MP2 energy difference for HSiOH, to estimate a wavelength close to 425 nm for the singlet-triplet transition of the silylene. The predicted transition is in a similar wavelength region to that estimated for the silylene $Si(OH)_2$. The transition energies for these isomers are summarized in Fig. 2.

Energetics of $Si(O)H(SiH_3)$. We have also substituted SiH_3 directly for H in $Si(O)H_2$ to form $Si(O)H(SiH_3)$. The singlet-triplet energy at the MP2/DZP level for this compound is 62.9 kcal/mol. This value is lowered to 62.2 kcal/mol when zero-point effects are included. An application of the usual correction factor leads to the prediction of a transition wavelength close to 499 nm for the adiabatic singlet-triplet transition.

Energetics of $Si(O)(SiH_3)_2$. The addition of a second SiH_3 group leads to $Si(O)(SiH_3)_2$ involving the bonding of two silicon atoms to a third. The singlet-triplet energy at the MP2/DZP level for this compound is 59.1 kcal/mol, which, with the zero-point correction, yields 58.8 kcal/mol. This value is lowered to 53.9 kcal/mol by applying the 4.9 kcal/mol correction factor outlined previously. We thus estimate an adiabatic singlet-triplet transition wavelength close to 530 nm.

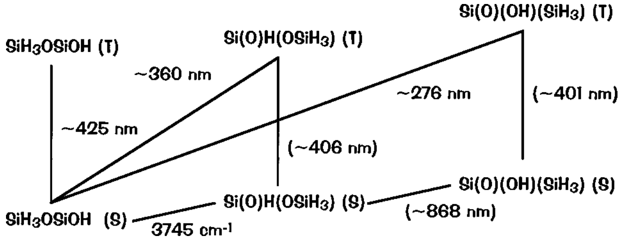

FIG. 2. Schematic of transition energies of the isomers $Si(O)H(OSiH_3)$, $Si(O)(OH)(SiH_3)$, and SiH_3OSiOH. All transition energies correspond to adiabatic transitions between minima of the ground and excited state potentials and include zero-point energy corrections. Values in parentheses are transitions that do not originate from the ground-state silylene.

Energetics of $Si(O)(SiH_3)(OSiH_3)$. Substitution of the H in $Si(O)H(OSiH_3)$ with an SiH_3 group leads to a slight redshift of 5 nm. A similar small redshift of 10 nm is predicted if SiH_3 is substituted for H on the OH in $Si(O)(OH)(SiH_3)$. The predicted transition for $Si(O)(OSiH_3)(SiH_3)$ is obtained from a singlet-triplet splitting of 75.7 kcal/mol at the MP2/DZP level, applying both a zero-point correction of 1.2 kcal/mol and the 4.9 kcal/mol correction factor outlined above. If $Si(O)(SiH_3)(OSiH_3)$ is considered to be formed from the insertion of an O into an Si-Si bond in $Si(O)(SiH_3)_2$, a much larger blueshift of 119 nm is predicted.

Tricoordinated silicon with a dangling electron. As we evaluate possible surface bound silicon-based emitters, we must also consider the possible contribution of tricoordinated silicon centers, SiXYZ, which possess a dangling electron. Excitations of the singly occupied electron or from fully occupied orbitals into its singly occupied orbital could occur at sufficiently low energies so that emission from the resulting excited states might contribute to the observed spectral features. We model this site with a silicon coordination ranging from SiH_3 to $Si(OH)_3$ with the progressive replacement of hydrogen by an OH ligand.

Geometries for SiH_3, $Si(OH)H_2$, $Si(OH)_2H$, and $Si(OH)_3$ were optimized at the DFT level as described previously. Vibrational frequencies were calculated to demonstrate that the structures correspond to minima.[43] Excited-state energies were calculated at these minimum geometries using the configuration interaction singles (CI-singles) method where the excited states are modeled as single excitations from the Hartree-Fock ground state.[44] Six states were determined by using this CI-singles approach. We first benchmarked the method with the molecule SiH_3, for which experimental data is available. The A-X transition for SiH_3 has been observed in the region 205–250 nm.[45] Energies were initially calculated with the augmented polarized triple ζ basis set (TZ2PF) described above for $Si(O)H_2$. The results are presented in Table VI. The lowest excitation energy is associated with a degenerate excitation at 204 nm (6.07 eV) located in the same region as the experimental spectrum. We then used a

TABLE VI. Calculated adiabatic transition wavelengths in nm and energies (eV) for SiXYZ silyl radicals. The symbol e after a transition denotes that it is doubly degenerate.

Molecule	Transition 1	Transition 2	Transition 3
SiH_3 (TZ2PF)	204 (6.07) e	198 (6.25)	197 (6.30) e
SiH_3	202 (6.14) e	196 (6.32) e	196 (6.34)
$Si(OH)H_2$	256 (4.84)	210 (5.91)	196 (6.33)
$Si(OH)_2H$	233 (5.33)	214 (5.80)	200 (6.19)
$Si(OH)_3$	200 (6.19)	196 (6.31)	187 (6.65)

smaller basis set, the polarized double ζ basis set described above, augmented by a diffuse function on H and a diffuse set of p functions on Si and O. For SiH_3, the excitation energy of the lowest-energy transition is predicted to be 202 nm (6.14 eV) in excellent agreement with the results obtained with the larger basis set. We thus have used this basis set for the remaining silyl radical calculations. The results catalogued in Table VI show that substitution of the first OH for H lowers the adiabatic transition energy to 4.84 eV (256 nm) but that subsequent substitution of the H by OH raises the transition energy. The full substitution of three OH's yields a transition energy of 6.19 eV (200 nm), essentially the same as that for SiH_3. These results suggest that SiXYZ radical species cannot account for the observed transitions.

Excited singlet-triplet energy splittings for silylenes. We have calculated the excited singlet-triplet energies for the silylene structures considered above and summarized in Table V. The electron configuration for the triplet state, which corresponds to an in-plane and out-of-plane p orbital valence combination can also be coupled as a singlet. To estimate the energy of the singlet, we make use of the geometry of the triplet, which is very close to that of the open-shell singlet, and calculate the triplet wave function at the restricted open-shell HF (ROHF) level. We then use this wave function to calculate the energy of the excited singlet at the two-configuration level for an open-shell singlet. For planar HSiOH we determine a value for this splitting of 44.9 kcal/mol in excellent agreement with our previous result of 44.6 kcal/mol. The planar structure for the triplet is not a minimum. This structure is 2.4 kcal/mol above the twisted structure at the MP2 level. Although we have not obtained convergence to the correct open-shell singlet state, the combination of results obtained for both HSiOH and HOSiOH (see below) suggest that the triplet-singlet open-shell splitting is not dependent on the torsion potential. Thus we can estimate that the open-shell singlet is 83.3 kcal/mol (343 nm) above the singlet ground state of the silylene. For the HOSiOH silylene, the planar structure for the triplet is 8.4 kcal/mol above the twisted structure. The singlet-triplet splitting for the planar structure is 61.9 kcal/mol whereas that for the twisted structure is 62.3 kcal/mol. We thus estimate that the open-shell singlet is 126.5 kcal/mol (158 nm) above the ground-state singlet. These calculated energies suggest that the silylene moiety is unlikely to be involved in the observed PS luminescence unless there are pathways for converting between the silylenes and the silanones.

Summary of energetics and substituent effects. We have found that the substitution of SiH_3 for H has only a small effect on the singlet-triplet transition energies for those model silicon oxyhydride compounds we have considered. A much larger effect results when H (or SiH_3) are replaced by an OH or $OSiH_3$ group leading to a significant blueshift for the singlet-triplet transition and a predicted adiabatic transition energy that (1) is very similar for each of the compounds and (2) is quite consistent with the observed peak in the porous silicon excitation (PLE) spectrum.

C. Frequencies

The calculated vibrational frequencies for $Si(O)H_2$ are given in Table VII. The assigned Si=O stretch is evaluated

TABLE VII. Vibrational frequencies (ν in cm^{-1}) and infrared intensities (I in km/mol) for the ground state of $Si(O)H_2$ at the MP2/DZP and DFT/TZVP levels and the excited-state triplet and singlet at the MP2/DZP level.

	Ground state				
Sym	ν DZP/MP2	I DZP/MP2	ν DFT/TZVP	I DFT/TZVP	Approximate assignments
a_1	2345	53	2127	23	Si-H sym str
	1182	55	1197	67	Si=O str
	1065	61	977	31	H-Si-H bend
b_1	2354	166	2132	102	Si-H asym str
	706	70	676	41	H-Si-H in-plane rock
b_2	728	80	693	35	out-of-plane bend
	Excited states				
	triplet (DZP/MP2)		singlet (DZP/MP2)		
a'	2275	38	2297	44	Si-H sym str
	929	84	930	88	H-Si-H bend
	860	122	854	139	Si=O str + H-Si-H bend
	745	25	760	24	out-of-plane bend (inversion)
a''	2311	134	2330	120	Si-H asym str
	534	42	691	80	H-Si-H in-plane rock

TABLE VIII. Vibrational frequencies (ν in $\mathrm{cm^{-1}}$) and infrared intensities (I in km/mol) for the ground-state $\mathrm{Si{=}O}$ stretches in the substituted silanones at the MP2/DZP and DFT/TZVP levels.

Molecule	ν	I	ν	I
	DZP/MP2		DFT/TZVP	
$\mathrm{Si(O)H_2}$	1182	55	1197	67
$\mathrm{Si(O)H(OH)}$	1244	135	1245	147
$\mathrm{Si(O)(OH)_2}$	1276	173	1275	194
$\mathrm{Si(O)H(OSiH_3)}$	1247	197	1245	185
$\mathrm{Si(O)(OH)(SiH_3)}$	1222	85	1224	117
$\mathrm{Si(O)H(SiH_3)}$	1150	26	1178	67
$\mathrm{Si(O)(SiH_3)_2}$	1125	17	1165	62
$\mathrm{Si(O)(SiH_3)(OSiH_3)}$	1225	126	1220	175

as 1182 $\mathrm{cm^{-1}}$ at the DZP/MP2 level and as 1197 $\mathrm{cm^{-1}}$ at the DFT/TZVP level. These values compare favorably with the frequencies measured by Withnall and Andrews[46] suggesting that only a minimal correction factor should be applied.

The $\mathrm{Si{=}O}$ stretching frequencies for the substituted silanones are given in Table VIII and all of the frequencies for the model compounds $\mathrm{Si(O)(OH)(SiH_3)}$ and $\mathrm{Si(O)(OSiH_3)(SiH_3)}$ are given in Table IX. The frequencies for the remaining compounds are reported in the supplementary material (see Ref. 71). The substitution of OH for H leads to an increase of 62 $\mathrm{cm^{-1}}$ in $\nu(\mathrm{Si{=}O})$ to 1244 $\mathrm{cm^{-1}}$ at the MP2/DZP level. When a second OH replaces hydrogen, this raises the $\mathrm{Si{=}O}$ stretching frequency by another 32 $\mathrm{cm^{-1}}$ to 1276 $\mathrm{cm^{-1}}$. The replacement of H with $\mathrm{SiH_3}$ in $\mathrm{Si(O)H_2}$ leads to a decrease of 30 $\mathrm{cm^{-1}}$ in the $\mathrm{Si{=}O}$ stretch, yielding a value of 1150 $\mathrm{cm^{-1}}$. The substitution of the hydroxyl H with $\mathrm{SiH_3}$ in $\mathrm{Si(O)H(OH)}$ to yield $\mathrm{Si(O)H(OSiH_3)}$ also does not change the $\mathrm{Si{=}O}$ stretch by more than a few $\mathrm{cm^{-1}}$; however, the substitution for the H on Si to yield the isomer, $\mathrm{Si(O)(OH)(SiH_3)}$, lowers the $\mathrm{Si{=}O}$ stretch by 22 $\mathrm{cm^{-1}}$. Substitution of the H on the OH in $\mathrm{Si(O)(OH)(SiH_3)}$ by $\mathrm{SiH_3}$ leads to only a very small change in the $\mathrm{Si{=}O}$ stretching frequency, an increase of 3 $\mathrm{cm^{-1}}$. Thus the changes in the ground-state $\mathrm{Si{=}O}$ stretch frequency upon substitution are modest and we expect to observe a reasonably intense $\mathrm{Si{=}O}$ stretch in the range of 1150–1275 $\mathrm{cm^{-1}}$.

As we compare the excited-state frequencies for $\mathrm{Si(O)H_2}$ given in Table VII with those of the ground state, we find only small differences between the frequencies of the triplet and excited-state singlet. We thus consider only the changes between the ground-state singlet and the excited-state triplet in the following discussion. The Si-H stretch in the excited-state triplet is predicted to decrease by between 50 and 75 $\mathrm{cm^{-1}}$ from that of the ground state. Most importantly, the $\mathrm{Si{=}O}$ stretch decreases significantly in the excited state from 1182 to 860 $\mathrm{cm^{-1}}$, consistent with the formation of a much longer Si-O excited state bond. The HSiH in-plane rock decreases by almost 200 $\mathrm{cm^{-1}}$. The only frequency that does not show a significant change is the out-of-plane bend. Similar comments can be made regarding the remaining silanones.

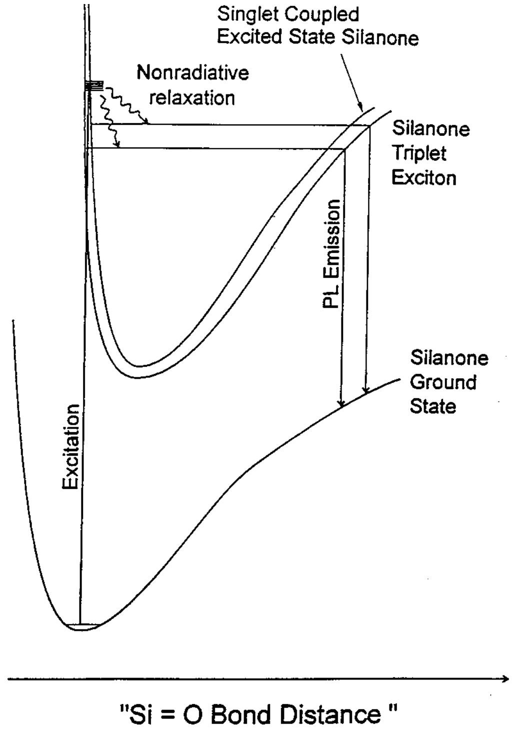

FIG. 3. Schematic diagram of silanone ground-state singlet and excited-state singlet and triplet potentials showing the origin of the substantial difference in photoluminescence excitation (PLE) and subsequent photoluminescence (PL) emission energies.

The silylene frequencies are given as supplementary material (see Ref. 71). The simplest silylene, HSiOH has an Si-O stretch at 860 $\mathrm{cm^{-1}}$ comparable to that of the excited triplet state of $\mathrm{Si(O)H_2}$. This stretching frequency changes very little in the excited triplet ($\sim$40 $\mathrm{cm^{-1}}$ increase). When OH groups form the silylene, the symmetric component of the Si-O stretch combines with the H-O-Si bend yielding a splitting close to 80 $\mathrm{cm^{-1}}$, the resulting bands being 904 and 824 $\mathrm{cm^{-1}}$. The asymmetric Si-O stretch combination is then at 881 $\mathrm{cm^{-1}}$, within the same frequency range as that found for HSiOH.

IV. DISCUSSION

The silanone-based oxyhydrides and the PS photoluminescence. The calculations outlined above provide significant insight into the electronic properties of the silanones and silylene-based oxyhydrides, their excitations, and their potential behavior as fluorophors, bound to a PS surface, which can be associated with the photoluminescence from porous silicon. We have broadly covered the types of substituents expected at an $\mathrm{Si{=}O}$ center on a silicon surface and we have included other potential types of molecular emitters such as silylenes and silyl radicals. Those ‘‘best-fit’’ silanone-based oxyhydride structures, the transitions of which are summarized in Table V, which contain either an $\mathrm{OSiH_3}$ or OH group bound to an $\mathrm{Si{=}O}$ functionality, all display adiabatic singlet-triplet separations in the range very close to 400 nm. Coupled with the large shift in the excited-state triplet versus ground-state singlet $\mathrm{Si{=}O}$ bond distances (outlined in Table II and diagrammed schematically in Fig. 3) and the expected similar character of the corresponding singlet-coupled silanone excited state, which lies only slightly higher in energy, these calculations predict that the maxima in the PLE spectrum corresponding to a vertical excitation at room temperature, from the lowest levels of the ground electronic singlet state to relatively higher vibrational levels of the low-lying triplet state, will be shifted to considerably shorter wavelength than the ~400-nm wavelength corresponding to the adiabatic energy separation. The peaking of the PLE (excitation) spectrum at ~350 nm, which has been observed by several researchers,[12,27] is therefore completely consistent with the expected behavior of the silanone-based oxyhydridelike fluorophors of the form O═Si(OH)- or O═Si($OSiH_3$)- bound to the PS surface. Further, the large shift in the excited triplet state should result in vertical transitions in emission that lead to a considerable redshift of the PL emission spectrum (~500–550, 600–800 nm) relative to the excitation wavelength, again completely consistent with observation.[5(a)] The calculated properties for the ground and low-lying triplet states of the silylenes are in distinct contrast. Not only are their singlet-triplet absorption spectra shifted to considerably longer wavelength but also they undergo (relatively) much smaller changes in bond length in the process of transition. Therefore, their absorption and emission spectra should be in very similar wavelength regions. We again emphasize that the locations of the silanone-based unsaturated silicon oxyhydride excited triplet states and the known peak wavelength of the porous silicon (PLE) excitation spectrum (~350 nm) (Ref. 27) both bear a clear resemblance to the known singlet-triplet splittings of the low-lying silicon monoxide intercombination band systems.[28]

The fluorophors that we suggest as possible sources of the porous silicon PL can represent localized centers that would be similar in form to the localized surface defects (or centers) associated by Prokes and co-workers[3,47] with the region of the PS surface from which the ''orange-red'' PL originates. Prokes and co-workers have considered and modeled the role of interfacial oxide-related defects in the form of nonbridging oxygen-hole centers (NBOHC's). These luminescent sources have also been suggested, more recently, by other researchers.[48]

The close coincidence of the geometries of the triplet exciton and the slightly higher-lying singlet-coupled configuration for the silanone-based silicon oxyhydrides suggests that a feasible explanation of the PL pumping mechanism may involve either a direct pump to a strongly mixed triplet (singlet) state or an intersystem crossing from the pumped singlet to the triplet.[5a] Whichever mechanism is operative, the formation of the excited-state triplet as monitored by ODMR (Refs. 16–18) will result in a significant change in the Si═O bond length. Further, we expect and have obtained evidence for a rapid nonradiative relaxation within the excited-state manifold.[5a,24] As emission from the excited triplet to the ground-state singlet occurs from regions more representative of the minimum-energy structure of the triplet, this emission will be significantly redshifted from the PS absorption region as the significant change in geometry leads to a termination of the vertical transition much higher up the ground-state singlet curve (Fig. 3). Whereas the present calculations demonstrate a significant change in the excited-state bonding relative to the ground state, localized largely in the Si═O bond, for the model compounds considered, changes in the Si-Si bond distance (Table III) (Ref. 24) are of much smaller order (0.005–0.03 Å) and will produce a much smaller shift in the observed emission spectrum. However, this does not preclude the observation of short progressions in the ground and excited state Si—Si stretching frequencies.

There are additional striking trends that can be inferred from the data in Tables II and V and experimental observations.[5a,24] Porous silicon displays a ''green'' luminescence during the early and intermediate stages of the etching process. The transformation from green to orange-red luminescence is easily followed.[4,5] The green and orange emitters appear to be distinct surface entities that are selectively excited by a variety of light sources.[5,24] Before drying, a freshly etched sample appears green under Hg lamp excitation but orange-red when excited by a KrF or ArF laser. After the PS sample matures in air for a considerable period, its transformation to an orange-red emitter is complete and all illuminated regions bear the orange-red luminescence *regardless of the uv excitation wavelength*. This suggests a chemical (oxidative) transformation.[5,24]

The green and orange-red emissions have been previously assigned to interlocking exciton fluorescence and phosphorescence emissions, respectively.[6,7] However, a series of *in situ* pump excitation experiments with nitrogen and KrF lasers and a Hg lamp[5,24] again suggest that the green and orange-red luminescence are related by chemical transformation and that the green emission emanates from a precursor state that is chemically transformed to the final orange-red emitter.[5] An intersystem crossing process between a short-lived singlet and a long-lived triplet, which correlate with these two emitters, as suggested by others,[6] does not correlate well with these recent experimental observations. Although the overlap of the emission ranges for the green and orange-red emitters prevents a ready evaluation of the radiative lifetime of the green emitter, its emission rate appears comparable to that for the long-lived orange-red emission feature.[5,24]

From Table II, we note that whenever an OH or $OSiH_3$ group is bound to the silicon involved in the silanone bond, the change, $\Delta r(\mathrm{SiO})$, is consistently of order 0.17 Å. Further, an additional OH group does little to affect this differential change in bond length accompanying the singlet-triplet transition. In the absence of an -OH or -$OSiH_3$ group this change is notably smaller, decreasing from 0.155 Å for $Si(O)H_2$ to 0.121 Å for $Si(O)(SiH_3)_2$. Thus, there are distinct differences associated with an -OR versus -R group bonded to the silicon. Further, we note (see Table V) the very similar adiabatic energy differences, $\Delta E \approx 3.05$ eV, which characterize those singlet-triplet transitions where an OH or OR group is bound to the Si═O bond. Contrast these virtually identical energy increments to the much lower and decreasing adiabatic energy differences associated with the series $Si(O)H_2$ ($\Delta r = 0.155$ Å), $Si(O)H(SiH_3)$ ($\Delta r = 0.142$ Å), and $Si(O)(SiH_3)_2$ ($\Delta r = 0.121$ Å) where the smaller change, $\Delta r(\mathrm{SiO})$, in the SiO bond length will lead to a smaller redshift of the PL emission feature. These results thus indicate that the oxyhydrides with bound -OR ligands will produce a much larger redshift of the PL emission spectrum relative to the peak of their PLE excitation spectrum than those fluorophors having only -R group ligand binding. We postulate that the magnitudes of these changes may be relevant to the correlation of the mechanism for PS formation with the assignment of the transforming green and final orange-red photoluminescence emissions.[15] We suggest that the green emitter is associated with an R group bound fluorophor and the orange emitter with the oxidative insertion into one or more SiH (—SiOH) or Si—SiH_x ($SiOSiH_x$) bonds.

Surface bound versus absorbed fluorophors. As we consider that the oxyhydride fluorophors are bound to the PS surface, they are to be distinguished from surface adsorbates. Sailor and co-workers[20,49–51] have obtained evidence for a wide diversity of effects as a PS surface is treated with several materials. While they have observed ''hole transfer'' quenching of the PL from PS by ferrocene[20] and the irreversible quenching due to aromatic hydrocarbons and redox active solutes,[49,50] they have also demonstrated[51] the reversible quenching of the PS luminescence in air due to trace levels of NO and NO_2 adsorbates. This suggests, as we have also observed,[5] a wide diversity of absorbant effects. The action of an adsorbate on a PS surface must be carefully distinguished from the creation or derivatization of a photoluminescent source.[52,53]

Colloidal silicon suspensions. The silane-based oxyhydride fluorophors that we consider not only are constituted from similar building blocks to those of ''annealed'' siloxene but also would appear to correlate with the photoluminescence from colloidal silicon particles in solution. Henglein and co-workers[54,55] have studied luminescent colloidal silicon particles prepared from HF-etched oxide-coated crystalline silicon ''nanoparticles'' formed in a manner similar to that outlined by Littau *et al.*[56] in the combustion of silane. These authors find that the orange-red PL can be activated by the aqueous HF etching of the silicon particles suspended in a 1:1 cyclohexane-propanol-2 solution in the presence of air. The required presence of oxygen (or traces of water vapor—under argon there is no luminescence) in these solution phase studies appears to indicate that the oxide layer created in the combustion of silane does not promote luminescence. Rather, as Fojtik *et al.* note,[54,55] the development of the orange-red. PL in nonpolar cyclohexane suggests that this original oxide layer must first be removed by HF. The silicon particles, with a nonpolar surface, are created in the cyclohexane phase. Here an equilibrium is established between their surface oxidation and reduction by O_2 and HF, respectively. Near-pristine silicon colloidal particles are formed whose oxidation, *to a much lower level than the original oxide coated particles*, produces luminescence. These authors suggest that the orange-red PL occurs when colloidal silicon particles carry only a limited component of oxidized centers and that the protonation state of these centers strongly affects the luminescence. This result is quite consistent with the formation of a silicon oxyhydride constituency with a required OH or OR ligand.

Infrared signatures. The calculated infrared frequencies for the silanones (Tables VII, VIII, and IX) are quite consistent with the range of infrared features observed by Xie *et al.*,[12] Dubin, Ozanam, and Chazalviel,[57] Hory *et al.*,[58] and, most recently, Mawhinney, Glass, and Yates.[59] All of the infrared studies indicate an oxidation signaling Si═O stretch region and the development of a feature in the $870-890\ \mathrm{cm}^{-1}$ range.[12,57–60] The silanones catalogued in Table VIII display calculated Si═O stretch regions in the range $1125-1247\ \mathrm{cm}^{-1}$ (see Ref. 46 for experimental data) and a dominant $870-900\ \mathrm{cm}^{-1}$ mode (see supplementary material[71]), which in the presence of an OH or $OSiH_3$ ligand appears to be associated, at least in part, with a combined Si═O stretch + H—Si-O (H-O-Si) bend, consistent with numerous observations.[12,21,57–59] However, we must note that Zacharias, Dimova-Malinouska, and Stutzmann[60] have studied the behavior of the 880-cm^{-1} band in hydrogenated amorphous silicon suboxide alloys. Based upon their finding a minimal dependence on deuteration, they ascribe the feature to a nonhydrogen-related origin. The assignment of this mixed mode feature has been reassessed by Mahwinney, Glass, and Yates,[59] and is clearly complex. Finally, we note the significant number of low-frequency modes associated with the exemplary silanones in Table IX (see also supplementary material[71]). We are especially drawn to the $\sim 130-150\ \mathrm{cm}^{-1}$ features, which not only are effectively associated with an Si-Si═O bend, likely present in an oxidizing PS environment, but also lie very close in energy to the transverse-acoustical (TA) phonon mode in bulk silicon.[61]

Tricoordinated silicon and the silylene isomers. It is clear from the calculated results that a tricoordinated silicon with a dangling electron cannot account for any of the uv-visible excitation and emission features that are associated with a PS surface. We have also considered the silylenes, which have an O bonded to the Si center. Here a direct singlet-triplet excitation is possible in the observed region but the oscillator strength of this transition will be extremely small. No direct excitation to an excited-state singlet can be correlated with the observed features as the singlet states lie at considerably higher energy and are therefore not accessible. Furthermore, we find that there are only two geometry changes on excitation to the triplet (see supplementary material[71]). The first involves a significant increase in the angle $<X\mathrm{Si}Y$ and the second is a torsion of $\sim 90°$ about the Si-O single bond. The latter has some energetic consequences but will not account for an observed significant redshift in emission. The only possible silylene geometry change that could account for this redshift is the 20–25° change in the angle $<X\mathrm{Si}Y$, but this has a much smaller energetic consequence than does the elongation of the Si═O bond in the silanone. Thus, it is quite unlikely that a silylene fluorophor corresponds to the moiety giving rise to the spectral features.

The *ab initio* electronic-structure calculations that we outline in this study point to another important general consideration, namely, that the characteristic absorption and emission features observed for porous silicon, if they are to be associated with a surface (moleculelike) based constituency, must involve unsaturated bonds. Dangling electrons as well as saturated bonding would be expected to produce species whose absorption and emission spectra lie in the deep ultraviolet. With this enjoinder, it would seem difficult to observe the emission features common to porous silicon from a completely hydrogen- or oxygen-passivated surface.

The question of quantum confinement. Recent studies of the photoluminescent emission from porous silicon as a function of excitation energy[24] support the conclusions of Kanemitsu *et al.*,[62] Prokes and Glembocki,[47] and Macauley *et al.*[63] that no obvious relationship exists between the PL spectrum and either the PLE spectrum or the evaluated particle size distribution on the PS surface. Kanemitsu *et al.*, in examining the relationship between particle size and PL peak

TABLE IX. Vibrational frequencies (ν in cm^{-1}) and infrared intensities (I in km/mol) for the ground-state silanones Si(O)(OH)(SiH$_3$) and Si(O)(OSiH$_3$)(SiH$_3$) at the MP2/DZP and LDFT/TZVP levels of theory.

Sym	ν DZP/MP2	I	ν DFT/TZVP	I	Approximate assignments[a]
			Si(O)(OH)(SiH$_3$)		
a'	3903	124	3670	117	O-H str
	2365	71	2190	25	SiH$_3$ str
	2337	51	2162	19	SiH$_3$ str
	1222	85	1224	117	Si$=$O str
	986	56	904	44	Si$=$O str+SiH$_3$ bend+H-O-Si bend
	938	96	894	10	Si-O str+SiH$_3$ bend+H-O-Si bend
	886	241	826	168	SiH$_3$ bend+H-O-Si bend
	836	219	810	198	SiH$_3$ bend$-$H-O-Si bend
	563	21	525	11	SiH$_3$ rock
	458	28	432	33	Si-Si str+SiH$_3$ bend+O-Si$=$O bend
	274	62	269	53	Si-Si str$-$O-Si$=$O bend
	148	2	154	0.7	Si-Si$=$O bend
a''	2350	74	2161	29	SiH$_3$ str
	987	55	907	17	SiH$_3$ bend
	550	18	510	2	SiH$_3$ rock
	487	172	449	172	H-O out of plane
	240	10	240	5	O,O,SiH$_3$ out of plane
	35	0.3	85	0.1	SiH$_3$ torsion
			Si(O)(OSiH$_3$)(SiH$_3$)		
a	2370	131	2198	47	(SiH$_3$)-Si (Si-H) str
	2365	67	2186	88	(SiH$_3$)-O (Si-H) str
	2364	136	2178	85	(SiH$_3$)-O (Si-H) str
	2359	78	2177	71	(SiH$_3$)-O (Si-H) str
	2347	70	2172	53	(SiH$_3$)-Si (Si-H) str
	2335	55	2167	28	(SiH$_3$)-Si (Si-H) str
	1225	126	1220	175	Si$=$O str
	1061	14	1031	382	Si-O-Si asym str
	1013	102	910	287	SiH$_3$O (inv) bend
	1011	211	898	34	SiH$_3$O (inv) bend
	1006	571	895	37	SiH$_3$O (inv) bend
	987	50	892	28	SiH$_3$-Si bend
	986	37	889	15	SiH$_3$-Si bend
	909	674	803	253	SiH$_3$ (inv) bend
	755	63	691	39	SiH$_3$(O) rock
	745	60	677	39	SiH$_3$(O) rock
	635	3	619	5	Si-O-Si sym str
	551	13	507	4	SiH$_3$(Si) wag
	547	7	483	21	SiH$_3$(Si) wag
	473	32	452	30	Si-Si str+Si-O-Si bend
	296	42	280	33	O-Si-O bend
	261	34	260	26	inversion at Si$=$O
	133	8	128	6	Si-Si-O bend
	83	0	110	1	Si-O-Si inversion
	65	4	95	2	SiH$_3$-Si torsion
	54	1	22	2	SiH$_3$-O torsion
	49	0	14	6	Si-O torsion

[a] Assignments based on DFT normal modes.

energy, have used optical absorption, Raman spectroscopy, and transmission electron microscopy to assess the partical size and photoluminescence. They find a blueshift in the optical absorption spectrum for particles decreasing in size from 9 to 2 nm but observe no change in the corresponding PL peak energy. This result conclusively demonstrates that the PL peak emission energy is not correlated with the particle size. Time-dependent laser excitation studies have suggested the manifestation of a pumping sequence between a ground state and a strongly shifted excited state as the pumped excited-state levels, high in the excited-state manifold, undergo nonradiative relaxation.[24] This cascade process leads to a redshifting of the PL emission spectra as a function of increasing time following optical excitation.[5,24,64] We also find that the behavior of the PL in air is quite similar regardless of the manner in which a sample is properly prepared.[5] These studies, in concert with the work of Prokes *et al.*[47] and Macauley *et al.*,[63] strongly argue against quantum confinement as a source of the PS photoluminescence.

Schuppler and co-workers[10,11] have performed an extensive study in which they establish a consistent structural picture of the species responsible for the PL from hydrogen-passivated PS and oxidized Si nanocrystals. These authors establish the silicon coordination and suggest that the average structures in PS are particles and not wires and that the relationship between peak luminescence energy and average particle size (strongly correlated with shape modeling) for the PS samples is very similar to that for Si nanocrystals. The authors demonstrate a lack of (Si-O) related x-ray absorption in freshly etched PS samples, which suggests the presence of little SiO_2 in distinct contrast to the SiO_2-coated nanocrystals produced in silane combustion.[56] This certainly appears to be consistent with the observations of Fojtik *et al.*[54,55] which suggest that the combustion-prepared, coated, nanocrystals must first be treated before they luminesce as colloidal suspensions.

By using near-edge x-ray-absorption fine structure (NEXAFS), Schuppler and co-workers[10,11] have established the coordination of silicon nearest neighbors, determining that the average number of first-nearest-neighbor Si atoms, N_{Si} in PS is notably less than the value of 4 established concurrently for amorphous and crystalline silicon. These authors suggest that the decrease in silicon nearest-neighbor coordination is due exclusively to hydrogen passivation; however, NEXAFS is unable to detect hydrogen directly and, thus, conclusively eliminate other possible coordinations to silicon. In correlation with the observations of Fojtik *et al.*[54,55] and others,[21,22,24] the possibility that these lower coordination numbers are associated with oxyhydride formation must be considered. Further, the very interesting correlations demonstrated by Schuppler and co-workers, if they are associated with a surface bound entity, might be associated not with particle size (modeled but not directly measured) but with an enhanced surface curvature and tension.

A number of researchers have recorded a blueshift in the PS photoluminescence emission spectrum that appears to parallel increasing etch effectiveness. The blueshift has been attributed to the creation of quantum-confined silicon particulates that decrease in size with increasing etch time; however, one might also attribute the observed changes to the role of surface curvature (tension) and structural strain as it influences the PL process by creating local force gradients. In fact, Unagami[65] has measured the intrinsic stress in porous silicon layers formed from in the aqueous HF etch, finding a macroscopic stress that extends from the compressive to tensile. Friedersdorf *et al.*[66] have observed the influence of stress on the PL of PS structures, correlating the blueshift in PL peak energy with surface microstructure. These authors conclude that the characteristic cellular structure occurring in high porosity films is due to high surface stresses. This cellular structure is not formed during the etching process itself but occurs during electrolyte evaporation after removal of the PS from solution. Enhanced surface tensions associated with increased curvature appear to be operative. Finally, in close agreement, Kanecko, French, and Wolffenbuttel[67] have very recently noted that, while an enhanced etching cycle leads to a blueshift in the PL spectrum, the high porosity structure created is clearly strained. Whereas these authors note that the observed blueshift suggests quantum effects, the surface state of the porous layer also is suggested to play an important role. This is certainly consistent with a surface bound silanone-based oxyhydride source for the PS luminescence as the oxyhydride is influenced by surface tension.

The replicates of phonon structure that have been reported for PS samples at 2 K by Calcott and co-workers[6–8] and most recently by Collins, Fauchet, and Tischler,[48] when exciting the PS surface over the wavelength range commensurate with the photoluminescence from PS, are certainly intriguing and may indicate the signature for bulklike crystallites existent on a PS surface at low temperatures. Only Suemoto *et al.*[68] have observed any semblance of this structure at temperatures exceeding 6 K (dependence of absorption edge structure at 78 K). However, the direct correlation of the suggested phonon structure observed at 2 K with the absorption edge recorded by several researchers and the photoluminescence that dominates the emission from PS at room temperature is tenuous. In fact, Rosenbauer *et al.*,[69] in carrying out an extensive study of the resonantly excited PL spectrum of PS, have suggested that two separate luminescence mechanisms are operative in PS. The very efficient process that dominates the usually observed (room-temperature) PL excited at energies generally in excess of 3 eV may well be distinct from that which is associated the phononlike structure that can be seen only at low temperatures when the commonly observed efficient mechanism is suppressed by excitation at energies lower than 2 eV.

Additional consideration of the long-wavelength phonon replicates observed at low temperatures reveals further difficulties. The arguments that Calcott and co-workers[6–8] have used to prove that quantum confinement accounts for the phonon replicates in PS relies on the observation of only *two* (momentum conserving) *phonon* replicates in the low-temperature spectrum, these features being attributed to Si transverse-optical (TO) phonons. However, several authors have observed a significantly richer structure in the long-wavelength spectrum. Suemoto *et al.*[68] have reported three or more phonon structures having an energy spacing close to 56 meV. It has also been shown by Rosenbauer *et al.*[69] that a minimum of four equally spaced phonon steps (including the zero-phonon line) all separated by 56.1 meV can be monitored in all of the samples that they have studied. This casts doubt on the proof of quantum confinement as espoused by Calcott and co-workers,[6,7] and makes more feasible the possibility of a surface bound or defect-related emission.

It is also worth noting that alternate explanations might be invoked to explain what appear to be features similar to the (TO) (Ref. 61) and transverse-acoustical (TA)[61,62] mode structure of bulk silicon. This structure, of course, is measured on the basis of energy shifts from an exciting laser frequency adjusted by the so-called exchange coupling factor

Δ,[6–8] which increases with excitation frequency.[70] This invokes some concern as Δ varies approximately from 10 meV ($\sim 80\ \mathrm{cm}^{-1}$) at 1.72 eV to 30.4 meV ($\sim 240\ \mathrm{cm}^{-1}$) at 2.1 eV.[24,70] This, of course, introduces a clear uncertainty into the measure of the frequency shifts from an exciting laser line as well as the meaning of onsets. However, even if we accept the application of this correction factor to the PLE spectra generated at 2 K, we are intrigued by the near matchup of the relevant silanone frequencies recorded in Table IX (and as supplementary material, see Ref. 71) and the frequency separations for the broad phonon features recorded by Calcott *et al.*[7] Specifically, the anticipated $\mathrm{Si\text{-}Si{=}O}$ bending frequency given in Table IX, $\sim 130–150\ \mathrm{cm}^{-1}$ is close to the TA-phonon frequency of bulk silicon. The Si-Si stretch frequency is of the order $450\ \mathrm{cm}^{-1}$ for the ground states of $\mathrm{Si(O)(OH)(SiH_3)}$ and $\mathrm{Si(O)(OSiH_3)(SiH_3)}$, changing little for the excited-state triplet. Not surprising is the close agreement between this frequency and that of the TO- ($\sim 511\ \mathrm{cm}^{-1}$) phonon mode frequency of a bulk silicon crystallite. Note also that the small change in the Si-Si bond distance is consistent with the observations by several authors.[6–8,68,69] of only a few ‘‘phonon satelites’’ in their photoluminescence emission spectra at 2 K. This structure might simply be ascribed to a short progression in a ground-state Si-Si stretch, thus rendering the arguments presented by Calcott *et al.*[6] concerning momentum conserving phonons extremely tenuous. The observed phonon replicates clearly require considerable further study.

ACKNOWLEDGMENTS

We gratefully acknowledge very helpful discussions with Dr. Sharka Prokes, and thank Professor Martin Stutzmann for providing us with data on his ODMR experiments. We acknowledge financial support from the Office of the President at the Georgia Institute of Technology under the auspices of the Focused Research Program. The quantum chemical calculations were performed under the auspices of the Office of Basic Energy Sciences, U.S. Department of Energy, under Contract No. DE-AC06-76RLO 1830 with Battelle Memorial Institute, which operates the Pacific Northwest National Laboratory.

---

[1] L. T. Canham, Appl. Phys. Lett. **57**, 1046 (1990).

[2] (a) Y. Kanemitsu, Phys. Rep. **263**, 1 (1995); (b) G. C. John and V. A. Singh, *ibid.* **263**, 93 (1995).

[3] S. M. Prokes, J. Mater. Res. **11**, 305 (1996).

[4] E. S. Astroua, S. V. Belov, A. A. Lebedev, A. D. Rermenjuk, and Yu V. Rud, Thin Solid Films **255**, 196 (1995).

[5] (a) J. L. Gole and D. A. Dixon, J. Phys. Chem. B **102**, 33 (1998); (b) J. L. Gole, F. Dudel, L. Seals, M. Reiger, P. Kohl, and L. Bottomley (unpublished).

[6] See, for example, P. D. J. Calcott, K. J. Nash, L. T. Canham, M. J. Kane, and D. Brumhead, J. Phys.: Condens. Matter **5**, L91 (1993).

[7] P. D. J. Calcott, K. J. Nash, L. T. Canham, M. J. Kane, and D. Brumhead, J. Lumin. **57**, 257 (1993).

[8] K. J. Nash, P. D. J. Calcott, L. T. Canham, and R. J. Needs, Phys. Rev. B **51**, 17 698 (1995).

[9] A. G. Cullis, L. T. Canham, and P. D. Calcott, J. Appl. Phys. **82**, 909 (1997).

[10] S. Schuppler, S. L. Friedman, M. A. Marcus, D. L. Adler, Y. H. Xie, F. M. Ross, Y. J. Chabal, T. D. Harris, L. E. Brus, W. L. Brown, E. E. Chaban, P. J. Szajowski, S. B. Christman, and P. H. Citrin, Phys. Rev. B **52**, 4910 (1995).

[11] S. Schuppler, S. L. Friedman, M. A. Marcus, D. L. Adler, Y. H. Xie, F. M. Ross, T. D. Harris, W. L. Brown, L. E. Brus, and P. H. Citrin, Phys. Rev. Lett. **72**, 2648 (1994).

[12] Y. H. Xie, W. L. Wilson, F. M. Ross, J. A- Mucha, E. A. Fitzgerald, J. M. Macauley, and T. D. Harris, J. Appl. Phys. **71**, 2403 (1992).

[13] (a) F. Koch, V. Petrova-Koch, T. Muschik, A. Nikolov, and V. Gavrilenko, in *Microcrystalline Semiconductors: Materials Science and Devices*, edited by P. M. Fauchet, C. C. Tsai, L. T. Canham, I. Shimizu, and Y. Aoyagi, MRS Symposia Proceedings No. 283 (Materials Research Society, Pittsburgh, PA, 1993), p. 197; (b) F. Koch, V. Petrova-Koch, and T. Muschik, J. Lumin. **57**, 271 (1993); (c) F. Koch, in *Silicon-Based Optoelectronic Materials*, edited by M. A. Tischler, R. T. Collins, M. L. Thewatt, and G. Abstreiter, MRS Symposia Proceedings No. 298 (Materials Research Society, Pittsburgh, PA, 1993), p. 222.

[14] F. Boulitrop and A. Cheneuas-Paule, J. Phys. (Paris) **43**, C1 (1982).

[15] (a) S. Prokes, O. J. Glembocki, V. M. Bermudez, R. Kaplan, L. E. Friedersdorf, and P. C. Pearson, Phys. Rev. B **45**, 13 788 (1992); (b) S. M. Prokes, J. Appl. Phys. **73**, 407 (1993).

[16] H. D. Fuchs, M. Rosenbauer, M. S. Brandt, S. Ernst, S. Finkbeiner, M. Stutzmann, K. Syassen, J. Weber, H. J. Queisser, and M. Cardona, in *Microcrystalline Semiconductors: Materials Science and Devices* (Ref. 13a), p. 203.

[17] M. Stutzmann, M. S. Brandt, M. Rosenbauer, H. D. Fuchs, S. Finkbeiner, J. Weber, and P. Deak, J. Lumin. **57**, 321 (1993).

[18] M. S. Brandt and M. Stutzmann, Solid State Commun. **93**, 473 (1995).

[19] J. L. Gole and D. A. Dixon, J. Phys. Chem. **101**, 8096 (1997).

[20] J. M. Lauerhaas, G. M. Credo, J. L. Heinrich, and M. J. Sailor, in *Light Emission from Silicon*, edited by S. S. Iyer, R. T. Collins, and L. T. Canham, MRS Symposia Proceedings No. 256 (Materials Research Society, Pittsburgh, 1992), p. 137.

[21] A. J. Steckl, J. Xu, H. C. Mogul, and S. M. Prokes, J. Electrochem. Soc. **142**, L69 (1995).

[22] J. Yan, S. Shih, K. H. Jung, D. L. Kwong, M. Kovar, J. M. White, B. E. Gnade, and L. Magel, Appl. Phys. Lett. **64**, 1374 (1994).

[23] F. Dudel, J. L. Gole, M. Reiger, P. Kohl, J. Pickering, and L. Bottomley, J. Electrochem. Soc. **143**, L164 (1996).

[24] F. Dudel, D. A. Dixon, D. R. Grantier, and J. L. Gole, Phys. Rev. B **56**, 2137 (1997).

[25] J. L. Gole and F. P. Dudel, J. Appl. Phys. **82**, 3125 (1997).

[26] F. P. Dudel and J. L. Gole, J. Appl. Phys. **82**, 802 (1997).

[27] See, for example, L. E. Brus, P. F. Szajowski, W. L. Wilson, T. D. Harris, S. Schuppler, and P. H. Citrin, J. Am. Chem. Soc. **117**, 2915 (1995).

[28] See, for example, G. J. Green and J. L. Gole, Chem. Phys. **100**, 133 (1985).

[29] R. J. Glinski, J. L. Gole, and D. A. Dixon, J. Am. Chem. Soc. **107**, 5891 (1985).

[30] D. A. Dixon and J. L. Gole, Chem. Phys. Lett. **125**, 179 (1986).

[31] T. Kudo and S. Nagase, Chem. Phys. Lett. **128**, 507 (1986).

[32] (a) J. Andzelm E. Wimmer, and D. R. Salahub, in *The Challenge of d and f Electrons: Theory and Computation*, edited by D. R. Salahub, and M. C. Zemer, ACS Symposium Series No. 394 (American Chemical Society, Washington, D.C., 1989), p. 228; (b) J. Andzelm in *Density Functional Theory in Chemistry*, edited by J. Labanowski and J. Andzelm (Springer-Verlag, New York, 1991), p. 155; (c) J. W. Andzelm and E. Wimmer, J. Chem. Phys. **96**, 1280 (1992).

[33] Gaussian 94, Revision B.2, M. J. Frisch, G. W. Trucks, H. B. Schlegel, P. M. W. Gill, B. G. Johnson, M. A. Robb, J. R. Cheeseman, T. Keith, G. A. Petersson, J. A. Montgomery, K. Raghavachari, M. A. Al-Laham, V. G. Zakrzewski, J. V. Ortiz, J. B. Foresman, J. Cioslowski, B. B. Stefanov, A. Nanayakkara, M. Challacombe, C. Y. Peng, P. Y. Ayala, W. Chen, M. W. Wong, J. L. Andres, E. S. Replogle, R. Gomperts, R. L. Martin, D. J. Fox, J. S. Binkley, D. J. Defrees, J. Baker, J. P. Stewart, M. Head-Gordon, C. Gonzales, and J. A. Pople (Gaussian Inc., Pittsburgh, PA, 1995).

[34] S. M. Prokes, Electrochem. Soc. Interface **3**, 41 (1994).

[35] N. Godbout, D. R. Salahub, J. Andzelm, and E. Wimmer, Can. J. Chem. **70**, 560 (1992).

[36] A. Komornicki and G. Fitzgerald, J. Phys. Chem. **98**, 1398 (1993), and references therein.

[37] (a) C. Møller and M. S. Plesset, Phys. Rev. **46**, 618 (1934); (b) J. A. Pople, J. S. Binkely, and R. Seeger, Int. J. Quantum Chem. Symp. **10**, 1 (1976).

[38] (a) T. H. Dunning, Jr. and P. J. Hay, in *Methods of Electronic Structure Theory*, edited by H. F. Schaefer III (Plenum, New York, 1977), Chap. 1; (b) A. D. McLean and G. S. Chandler, J. Chem. Phys. **72**, 5639 (1980).

[39] (a) R. J. Bartlett, J. Phys. Chem. **93**, 1697 (1989); (b) S. A. Kucharski and R. J. Bartlett, Adv. Quantum Chem. **18**, 281 (1986); (c) P. J. Bartlett and J. F. Stanton, in *Reviews of Computational Chemistry*, Vol. V, edited by K. B. Lipkowitz and D. B. Boyd (VCH, New York, 1995), Chap. 2, p. 65.

[40] For the Si basis see K. D. Dobbs and D. A. Dixon, J. Phys. Chem. **98**, 5290 (1994); For O and H see K. D. Dobbs, D. A. Dixon, and A. Kormonicki, J. Chem. Phys. **98**, 8852 (1993).

[41] M. E. Colvin, R. S. Grev, H. F. Schaefer III, and J. Bicerano, Chem. Phys. Lett. **99**, 399 (1983).

[42] H. B. Schlegel, J. Chem. Phys. **84**, 4530 (1986).

[43] The structure of Si(OH)$_3$ showed a small imaginary frequency for the torsion about an Si-O bond.

[44] J. B. Foresman, M. Head-Gordon, J. A. Pople, and M. J. Frisch, J. Phys. Chem. **96**, 135 (1992).

[45] M. E. Jacox, J. Phys. Chem. Ref. Data Monogr. **3**, 127 (1994).

[46] R. Withnall and L. Andrews, J. Phys. Chem. **89**, 3261 (1985).

[47] (a) S. M. Prokes and O. J. Glembocki, Phys. Rev. B **49**, 2238 (1994); (b) S. M. Prokes, W. E. Carlos, and O. J. Glembocki, *ibid.* **50**, 17 093 (1994); (c) W. E. Carlos and S. M. Prokes, J. Appl. Phys. **78**, 2129 (1995); (d) S. M. Prokes and W. E. Carlos, *ibid.* **78**, 2671 (1995).

[48] R. T. Collins, P. M. Fauchet, and M. A. Tischler, Phys. Today **50**(1), 24 (1997).

[49] T. F. Harper, A. V. Gamboa, and M. J. Sailor, *Abstracts of the American Chemical Society 209th Annual Meeting, 1995* (American Chemical Society, Washington, D. C. 1995), p. 127.

[50] M. J. Sailor, J. L. Heinrich, and J. M. Lauerhaas, Stud. Surf. Sci. Catal. **103**, 209 (1997).

[51] J. Harper and M. J. Sailor, Anal. Chem. **68**, 3713 (1996).

[52] M. Warnjtes, C. Vieillard, F. Ozanam, and J. N. Chazalviel, J. Electrochem. Soc. **142**, 4138 (1995).

[53] E. J. Lee, J. S. Ha, and M. J. Sailor, in *Microcrystalline and Nanocrystalline Semiconductors*, edited by R. W. Collins, C. C. Tsai, M. Hirose, F. Koch, and L. Brus, MRS Symposia Proceedings No. 358 (Materials Research Society, Pittsburgh, PA, 1995), p. 387.

[54] A. Fojtik and A. Henglein, Chem. Phys. Lett. **221**, 363 (1994).

[55] A. Fojtik, M. Giersig, and A. Henglein, Ber. Bunsenges. Phys. Chem. **97**, 1493 (1993).

[56] K. A. Littau, P. J. Szajowski, A. J. Muller, A. R. Kortan, and L. E. Brus, J. Phys. Chem. **97**, 122 (1993).

[57] V. M. Dubin, F. Ozanam, and J. N. Chazalviel, Thin Solid Films **255**, 87 (1995).

[58] M. A. Hory, R. Herino, M. Ligeon, F. Muller, F. Gaspard, I. Mihalcesu, and J. C. Vial, Thin Solid Films **255**, 200 (1995).

[59] D. B. Mawhinney, J. A. Glass, Jr., and J. T. Yates, Jr., J. Phys. Chem. B **101**, 1202 (1997).

[60] M. Zacharias, D. Dimova-Malinouska, and M. Stutzmann, Philos. Mag. B **73**, 799 (1996).

[61] (a) P. J. Dean, J. R. Haynes, and W. F. Flood, Phys. Rev. **161**, 711 (1969); (b) K. L. Shakle and R. E. Nahory, Phys. Rev. Lett. **24**, 942 (1970); (c) T. Nishino, M. Takeda, and Y. Hamakawa, Solid State Commun. **14**, 627 (1974).

[62] (a) Y. Kanemitsu, H. Uto, Y. Matsumoto, T. Futagi, and H. Mimura, Phys. Rev. B **48**, 2827 (1993); (b) Y. Kanemitsu, H. Uto, Y. Matsumoto, T. Futagi, and H. Mimura, Jpn. J. Appl. Phys., Part 1 **32**, 411 (1993).

[63] J. M. Macauley, F. M. Ross, P. C. Searson, S. K. Sputz, R. People, and L. R. Friedersdorf, in *Light Emission from Silicon* (Ref. 20), p. 47.

[64] R. Laiho, A. Pavlov, and T. Tsuboi, J. Lumin. **57**, 89 (1993).

[65] T. Unagami, J. Electrochem. Soc. (to be published).

[66] L. E. Friedersdorf, P. C. Searson, S. M. Prokes, O. J. Glembecki, and J. M. Macauley, Appl. Phys. Lett. **60**, 2285 (1992).

[67] H. Kanecko, P. J. French, and R. F. Wolffenbuttel, J. Lumin. **57**, 101 (1993).

[68] T. Suemoto, K. Tanaka, A. Nakajima, and T. Itakura, Phys. Rev. Lett. **70**, 3659 (1993).

[69] M. Rosenbauer, S. Finkbeiner, E. Bustarret, J. Weber, and M. Stutzmann, Phys. Rev. B **51**, 10 539 (1995).

[70] Calcott *et al.* (Refs. 6 and 7) suggest that, to a reasonable approximation, $\Delta \sim (h\omega_p - E_{\mathrm{gap}})^{1.5}$, where $E_{\mathrm{gap}} = 1.17$ eV is the 2 K band-gap energy of bulk silicon and a calculation at $h\omega_p = 1.72$ eV fixes the constant of proportionality. At 2.1 eV, this gives (const=33.9) $\Delta = 30.4$ meV; at 3.5 eV, the peak of the PLE spectrum, we find $\Delta = 121$ meV. The implied Δ at room temperature would increase slightly to 125 meV *if the constant of proportionality holds over the range 2–300 K.*

[71] See AIP Document No. -EPAPS:E-PRBMD-57-08619 for additional tables. E-PAPS document files may be retrieved free of charge from our FTP server (http://www.aip.org/epaps/epaps.html) or from ftp.aip.org in the directory /epaps/. For further information: e-mail: PAPS@aip.org or fax: 516-576-2223.